Journal of Bioenergetics and Biomembranes, Vol. 27, No. 5, 1995

Original Article

Decoupling of the *bc*1 Complex in *S. cerevisiae*; Point Mutations Affecting the Cytochrome *b* Gene Bring New Information about the Structural Aspect of the Proton Translocation

Christophe Bruel,[1] Stephen Manon,[2] Martine Guérin,[2] and Danielle Lemesle-Meunier[1,3]

Received March 13, 1995; revised July 10, 1995; accepted July 10, 1995

Four mutations in the mitochondrial cytochrome *b* of *S. cerevisiae* have been characterized with respect to growth capacities, catalytic properties, ATP/$2e^-$ ratio, and transmembrane potential. The respiratory-deficient mutant G137E and the three pseudo-wild type revertants E137 + I147F, E137 + C133S, and E137 + N256K were described previously (Tron and Lemesle-Meunier, 1990; Di Rago *et al.*, 1990a). The mutant G137E is unable to grow on respiratory substrates but its electron transfer activity is partly conserved and totally inhibited by antimycin A. The secondary mutations restore the respiratory growth at variable degree, with a phosphorylation efficiency of 12–42% as regards the parental wild type strain, and result in a slight increase in the various electron transfer activities at the level of the whole respiratory chain. The catalytic efficiency for ubiquinol was slightly (G137E) or not affected (E137 + I147F, E137 + C133S, and E137 + N256K) in these mutants. Mutation G137E induces a decrease in the ATP/$2e^-$ ratio (50% of the W.T. value) and transmembrane potential (60% of the W.T. value) at the *bc*1 level, whereas the energetic capacity of the cytochrome oxidase is conserved. Secondary mutations I147F, C133S, and N256K partly restore the ATP/$2e^-$ ratio and the transmembrane potential at the *bc*1 complex level. The results suggest that a partial decoupling of the *bc*1 complex is induced by the cytochrome *b* point mutation G137E. In the framework of the protonmotive Q cycle, this decoupling can be explained by the existence of a proton wire connecting centers P and N in the wild type *bc*1 complex which may be amplified or uncovered by the G137E mutation when the *bc*1 complex is functioning.

KEY WORDS: ATP synthesis; transmembrane potential; decoupling; cytochrome *b*; mutants; revertants.

INTRODUCTION

It is now widely accepted that the link between the oxido-reduction reactions catalyzed by the *bc*1 complex and the electrogenic proton translocation across the membrane occurs according to a mechanism known as the protonmotive Q-cycle (Mitchell, 1975, 1976; Crofts and Wraight, 1983; Crofts, 1985; Trumpower, 1990a, b; Brandt and Trumpower, 1994). The electrochemical gradient generated across the membrane during this process may subsequently be used to drive ATP synthesis through the F_1-F_0 ATP synthetase complex or other energy-requiring reactions of the mitochondria, such as ion transport.

All the cytochrome *bc*1 complexes contain four redox prosthetic groups: a two-heme cytochrome *b*, a one-heme cytochrome *c*1, and a 2Fe-2S cluster protein. The mitochondrial cytochrome *bc*1 complexes contain additional subunits which are not essential to the Q-

[1] Laboratoire de Bioénergétique et Ingénierie des Protéines, C.N.R.S, 31 Chemin Joseph Aiguier, 13402 Marseille Cedex 20, France.
[2] Institut de Biochimie et Génétique Cellulaire, C.N.R.S, 1 rue Camille Saint Saëns, 33077 Bordeaux Cedex, France.
[3] To whom correspondence should be addressed.

0145-479X/95/1000-0527$07.50/0

cycle mechanism (Trumpower, 1990; Yang and Trumpower, 1986, 1988). The Q-cycle proposes that oxidation of ubiquinol into an unstable semiquinone leads to the transfer of one electron to the iron-sulfur protein with a release of two protons on the positive side of the membrane; the semiquinone is in turn rapidly oxidized by the low-potential cytochrome *b* heme *b*L. These two coupled steps of ubiquinol oxidation occur at a site near the positive side of the membrane which is referred to as center P (or QP site). Therefore, the two electrons from ubiquinol follow separate pathways: one electron is transferred to cytochrome *c* via the iron-sulfur cluster and cytochrome *c*1, the second is transferred from heme *b*L to the high-potential heme *b*H, localized on the opposite side of the membrane, and is recycled via a quinone molecule to form a stable semiquinone anion at a site referred to as center N (or QN site). An additional turnover of the cycle is necessary to reduce this semiquinone into ubiquinol. Thus, a complete Q-cycle sequence involves the oxidation of two ubiquinol molecules at center P, the reduction of only one molecule of ubiquinone into ubiquinol at center N, the reduction of two molecules of cytochrome *c*, the deposit of four protons on the positive side of the membrane, and the consumption of two protons on the negative side.

The eight membrane-spanning α helices cytochrome *b* (Rao and Argos, 1986; Crofts *et al.*, 1987; Brasseur, 1988) can be reduced through the center P and N pathways which are the targets of specific inhibitors (for review see Link *et al.*, 1993), the MOA type inhibitors exemplified by myxothiazol and the antimycin type inhibitor, respectively. The protonation/deprotonation events associated with the Q-cycle oxido-reduction reactions occurring at centers N and P require proton conductive pathways which link the bulk phase to these centers (Trumpower, 1990b); these pathways could involve protonic amino acid residues from cytochrome *b* (Trumpower, 1990b; Brandt and Trumpower, 1994b).

One important characteristic of the protonmotive Q-cycle mechanism lies in the obligatory coupling between electron transfer and proton translocation; its mechanistic stochiometry can only be modified in a way which would decrease the H^+/e^- ratio by 50% (Trumpower, 1990b; Beattie, 1993; Brandt and Trumpower, 1994). This would occur in some particular cases in which both electrons generated by ubiquinol oxidation would be transfered to cytochrome *c* via the iron-sulfur protein and the cytochrome *c*1; the recycling of one electron through cytochrome *b* would therefore be prevented, the center N pathway would be bypassed, and the resulting electron transfer would be antimycin insensitive.

DCCD[4] has been shown to block proton translocation without affecting electron transfer in the *bc*1 complexes (Beattie and Villalobo, 1982; Clejan and Beattie, 1983; degli Esposti, 1983; Beattie and Marcelo-Baciu, 1991; Beattie, 1993) and to bind to the aspartic acid residue located at position 160 in the yeast cytochrome *b* protein and to both aspartic acid and glutamic acid residues located at positions 155 and 166 in the spinach cytochrome *b*6, respectively (Beattie and Clejan, 1982; Beattie *et al.*, 1984; Wang and Beattie, 1991; Beattie, 1993). All these residues belong to the extramembranous amphiphatic loop which connects the transmembrane α helices 3 and 4 on the positive side of the membrane. This DCCD effect has been explained by conformational changes which would lead to a distorted quinol-oxidizing site that forces both electrons from ubiquinol to sequentially reduce the iron-sulfur protein (Beattie, 1993). An alternate path induced by the binding of DCCD to Asp160 and which might allow the proton to return to the negative side of the membrane has also been proposed (Brandt and Trumpower, 1994).

We described recently a novel class of cytochrome *b* mutants exhibiting appreciable electron transfer activity despite their inability to grow on respiratory substrates. This suggested that the redox-linked energy wastage observed in these mutants arise from a decoupling of proton translocation from electron transfer induced by the mutations (Tron and Lemesle-Meunier, 1990; Lemesle-Meunier *et al.*, 1993). Several pseudo wild type revertants have been obtained from these mutants (di Rago *et al.*, 1990a; di Rago *et al.*, 1990b; Coppée *et al.*, 1994). We report here on biochemical studies carried out on one of these mutants (G137E) and three of its revertants (E137 + I147F, E137 + C133S, and E137 + N256K) for which the second mutation partly restores the respiratory growth capacities of the corresponding strains. The analysis of our results suggests that the observed decoupling is not due to a mechanistic H^+/e^- variable stochiometry of the *bc*1 complex but to a backpass of the protons from the P side to the N side of the membrane that occurs through a proton wire which is associated to a functioning complex and uncovered by the mutations.

[4] Abbreviations used: DBH2, reduced 2,3-dimethoxy-5-methyl-6-decyl-1,4 benzoquinone; DCCD, dicyclohexylcarbodiimide; $ClPhzC(CN)_2$, carbonyl cyanide *m*-chlorophenylhydrazone.

EXPERIMENTAL PROCEDURES

Strains

The *rho*$^+$, *mit*$^-$ cytochrome *b* mutant 777-3A/M4871 was isolated from the haploid strain *rho*$^+$, *mit*$^+$ 777-3A α, *ade1*, *op1* (Kotylak and Slonimski, 1977). The nuclear recessive *op1* mutation impairs mitochondrial ATP/ADP translocation, which leads to the loss of the ability to grow on respiratory substrates even in the presence of a functional respiratory chain (Kovac *et al.*, 1967). Therefore, the cytochrome *b* mutant and its parental strain were crossed with the rho° strain KL14-4A/60 which possesses the wild type allele of the *op1* mutation (a, *his1*, *trp2*, OP1). By construction, the resulting diploid strains are all isogenic except for the cytochrome *b* mutations. All the experiments were carried out on the diploid strains. In the mutant, glycine 137 is replaced by glutamic acid (G137E) (Tron and Lemesle-Meunier, 1990). The revertants were isolated on glycerol medium (2% glycerol, 1% yeast extract, 1% bactopeptone) and were characterized previously (di Rago *et al.*, 1990b).

Media, Growth Conditions, and Preparation of Mitochondria

Media, growth conditions, and glass bead preparation of mitochondria were as described in Meunier-Lemesle *et al.* (1980). Helicase preparation of mitochondria was performed as described in Guérin *et al.* (1979).

Determination of Growth Yields

Growth yields were measured as described in a previous paper (Chevillotte-Brivet and Meunier-Lemesle, 1980).

Enzymatic Assays

Ethanol-oxidase, D-lactate-oxidase, and ethanol-ferricyanide oxido-reductase activities were measured in 0.65 M mannitol, 0.36 mM EDTA, 10 mM Tris-maleate buffer, and 0.3% bovine serum albumin, 4 mM Pi, pH 6.8. The oxygen consumption was recorded on a Gilson oxygraph in the presence of 1% ethanol or 10 mM D-Lactate. The ethanol-ferricyanide oxido-reductase activities were recorded on an Aminco DW2 spectrophotometer, in the dual-wavelength mode, by monitoring the reduction of ferricyanide at 420–470 nm in the presence of 4 mM KCN and 1,2 mM ferricyanide. The DBH2-cytochrome *c* oxidoreductase activities were recorded by monitoring the reduction of cytochrome *c* at 550–540 nm in 50 μM EDTA, 50 mM phosphate buffer, pH 7.4, 4 mM KCN, and 40 μM cytochrome *c*.

Kinetic Reduction of Cytochromes

Mitochondrial membranes were diluted to a concentration of 0.5 μM cytochrome *b*562 in 0.65 M sorbitol, 10 mM KH_2PO_4, 2mM EDTA, 0.1 mM $MgCl_2$ buffer, and 0.3% bovine serum albumin, pH 6.5. Antimycin and myxothiazol were prepared in ethanol and added to a final concentration of 20 and 30 μM, respectively. Succinate was added to a final concentration of 40 mM.

ATP Synthesis Measurement

Rates of ATP synthesis were determined simultaneously to substrate oxidation measurements under the same conditions (see the Enzymatic Assays section). [^{32}P]Pi (specific activity about 1000 cpm/nmol) was added at 4 mM. ATP synthesis was initiated by ADP addition (1 mM) and 0.1 ml aliquots were taken up at different times into 0.05 ml 3 M TCA. After centrifugation, phosphate was precipited according to the method of Sujino and Miyoshi (1964), and the radioactivity incorporated into ATP was counted on the supernatant. ATP synthesis was linear vs. time between 60 and 120 sec.

Transmembranous Electrical Potential Measurement

$\Delta\Psi$ was measured as the red shift of the absorbance spectrum of Rhodamine 123 following its matricial accumulation (Emaus *et al.*, 1986). Mitochondria (0.33 mg/ml) were suspended in the basal medium added with 0.33 μg/ml Rhodamine 123. $\Delta\Psi$ coupled to ethanol-oxidase, D-Lactate oxidase, and ethanol-ferricyanide oxido-reductase activities was measured under the conditions described above (see the Enzymatic Assays section). Rhodamine 123

absorbance was measured on an Aminco DW2 spectrophotometer at 524 nm vs. 499 nm. The absorbance signal was calibrated from diffusion potentials created by valinomycin (0.4 μg/ml) in the presence of KCl as follows: mitochondria were suspended in the absence of any respiratory substrate and in the presence of a range of KCl concentrations (0.1–100 mM). After the stabilization of the signal, valinomycin was added rapidly. The variation of the absorbance was extrapolated at the time of addition of the ionophore. This absorbance value was then plotted versus the transmembrane potential calculated from the Nernst equation assuming an internal (matricial) K^+ concentration of 120 mM. The signal vs. $\Delta\Psi$ curve was linear between 80 and 220 mV (negative inside).

RESULTS

Cell Growth, Mitochondrial Electron Transfer Activities, Inhibitor Titration, and Cytochrome Spectra Analysis

The parental wild type strain (W.T. strain), mutant G137E, and revertants G137E+I147F, G137E+C133S, and G137E+N256K were grown on 0.1, 0.2, 0.3, 0.4, and 0.5% galactose at 28°C in order to determine their growth characteristics (Fig. 1). The growth on 0.5% galactose results from, first, an approximately 15-h mainly fermentation phase during which the various strains all grew at the same rate and then a respiration phase during which no growth of respiratory-deficient mutants lacking *bc*1 complex activity occurred (Tron and Lemesle-Meunier, 1990). As shown in Fig. 1b, the growth associated with the respiratory phase was almost abolished in mutant G137E, severely affected in revertant G137E+I147F, and partially affected in revertants G137E+C133S and G137E+N256K; their growth rates (1/generation time) were 1, 4.6, and 7.5% of the W.T. strain value, respectively. The growth yield was severely affected in revertant G137E+I147F (20% of the W.T. value), and the revertants G137E+C133S and G137E+N256K exhibited an intermediate growth yield (40 and 50%, respectively) as compared with those of the mutant and the W.T. strain counterparts (values calculated from Fig. 1a).

The mitochondria were isolated from the mutant, the revertants, and the W.T. strain using the helicase preparation method, and their electron transfer activities were measured under steady state 3 (+ADP), 3u (+ClPhzC$(CN)_2$), and steady state 4 (static head) conditions (Table I). Although the G137E mutation abolished the growth on nonfermentable substrate, the mitochondria isolated from the mutant exhibited a 20% state 3 and state 4 respiration as compared with that of the W.T. strain. Under state 3u, the mutant ethanol oxidase activity was found to be 30% as compared with that of the W.T. strain. The secondary mutations C133S, I147F, and N256K, which partially restored the growth on nonfermentable carbon sources, slightly improved the electron transfer activity up to 30% of the corresponding W.T. strain level; the respiratory activities were completely inhibited by antimycin A in the W.T. strain, as well as in the revertants and the mutant. The G137E mutation was found not to interfere with the antimycin A binding site (Tron and Lemesle-Meunier, 1990) and to lead to a resistance toward myxothiazol corresponding to a twentyfold increase in the I_{50} value over that of the W.T. strain (Bruel and Lemesle-Meunier, 1993). The cytochrome *b*H red shift induced by antimycin A was conserved in all the strains. The secondary N256K mutation did not change this resistance toward myxothiazol (Giessler *et al.*, 1994), whereas the C133S mutation decreased this resistance fourfold (Bruel and Lemesle-Meunier, 1993). No significant difference in the level of synthesis of the various cytochromes was observed.

Theoretically, the level of the electron transfer activity of the mutant G137E should suffice for the strain to be able to grow; this strain did not, however, grow on respiratory substrate, and grew on galactose as a strongly decoupled strain. This paradox was further investigated by determining the ATP/$2e^-$ ratio and the transmembrane potential values associated with the complete electron transfer chain and with the functionally isolated *bc*1 and cytochrome oxidase complexes.

Determination of the ATP/$2e^-$ Ratio

The yeast *S. cerevisiae* was found to contain only two phosphorylation sites, which are associated with the *bc*1 and the cytochrome oxidase complexes (Ohnishi *et al.*, 1966). When ethanol and oxygen are used as substrates, the mitochondrial electron transfer involves both of these complexes. When D-lactate and oxygen are used as substrates in the presence of antimycin A, only cytochrome oxidase is involved whereas the *bc*1 complex alone intervenes in the electron transfer when ethanol and ferricyanide are used as substrates in the presence of KCN.

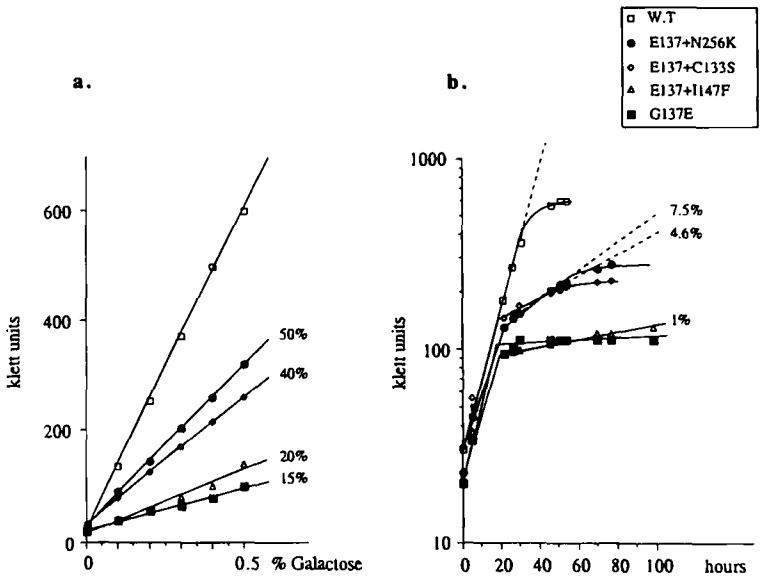

Fig. 1. Growth characteristics of the wild type strain (W.T.), mutant G137E, and revertants E137+C133S, E137+I147F, and E137+N256K. (a) Yeast cells were grown at 28°C on 0.1, 0.2, 0.3, 0.4, and 0.5% galactose in liquid medium and the optical density was recorded during the growth using a Klett densitometer. At each galactose concentration and with each strain, the maximum value of the growth was plotted versus the substrate percentage; this plot gives the growth yield. (b) The 0.5% galactose growth curve was plotted using a *Y*-axis logarithmic scale. The first 15 h or so corresponds to a mainly fermentative growth phase, whereas the second phase consists mainly of respiratory growth; the growth rate of each strain was calculated from the second-phase slopes. The mutant growth yields and growth rates are given as percentages of the wild type values. For the W.T. strain the growth yield was 95 g dry weight/mol substrate and the growth rate was 0.4 h^{-1}. The calibrations were such that 100 Klett units corresponds to 0.44 mg dry weight/ml.

ATP synthesis was measured under state 3 (ADP) conditions in the mutant, as well as in the revertant and W.T. strains using ethanol and oxygen as substrates (Table II). A decrease of 50% in the ATP/2e^- ratio was observed in the mutant G137E as compared with the W.T. strain. The secondary mutations C133S,

Table I. Electron Transfer Activities[a]

Strains	EtOH→O_2 State 3	EtOH→O_2 State 4	EtOH→O_2 State 3u	Lactate →O_2	EtOH→ ferricyanide
W.T.	91	49	97	29	145
G137E	18	10	29	27.5	45
E137+I147F	20	13	25	40	40
E137+C133S	25	15	29	nd	nd
E137+N256K	27	14	41	27	59

[a] The ethanol oxygen reductase, the D-lactate oxygen reductase (in the presence of antimycin A), and the ethanol ferricyanide reductase (in the presence of KCN) activities were measured in mitochondria isolated from the parental wild type strain (W.T.), the mutant G137E, and the three revertants E137+I147F, E137+C133S, and E137+N256K. The ethanol oxygen reductase activity (expressed in nmol O_2 $min^{-1} \cdot mg^{-1}$) was recorded under State 3 (in the presence of ADP), State 4, and State 3u (in the presence of $ClPhzC(CN)_2$) conditions. The D-lactate oxygen reductase activity is expressed in nmol $O_2 \cdot min^{-1} \cdot mg^{-1}$ and the ethanol ferricyanide reductase activity in nmol ferricyanide $\cdot min^{-1} \cdot mg^{-1}$. The respiratory medium was as follow: 0.65 M sorbitol, 10 mM KH_2PO_4, 2 mM EDTA, 0.1 mM $MgCl_2$, and 0.3% bovine serum albumin, pH 6.5.

Table II. Measurement of the ATP/$2e^-$ Ratio[a]

Strains	EtOH→O_2	Lactate→O_2	EtOH→ferricyanide
W.T.	1.2	0.56	0.65
G137E	0.6	0.5	0.28
E137+I147F	0.78	0.5	0.32
E137+C133S	0.72	n.d.	n.d.
E137+N256K	0.78	n.d.	0.43

[a] ATP synthesis experiments were carried out on mitochondria isolated from the wild type strain (W.T.), mutant G137E, and revertants E137+C133S, E137+I147F, and E137+N256K. Ethanol and oxygen or D-lactate and oxygen in the presence of antimycin A or ethanol and ferricyanide in the presence of KCN were used as substrates in order to investigate the coupling properties of the whole respiratory chain, the cytochrome oxidase alone, and the *bc*1 complex alone, respectively.

I147F, and N256K improved the mutant P/O ratio by 10–20%. The ATP/$2e^-$ ratio measured in the W.T. strain using D-lactate and oxygen as substrates in the presence of antimycin A was half of that obtained using ethanol as electron donor, which is consistent with the presence of only one phosphorylation site involved in D-lactate oxidation; under these conditions, no significant difference was observed between the ATP/$2e^-$ ratios determined in the mutant, the revertants, and the W.T. strain. Similar results were obtained in the absence of antimycin A. Lastly, the *bc*1 complex alone was investigated from the point of view of its coupling properties, using ethanol and ferricyanide as substrates in the presence of KCN. Under these conditions, a decrease of 55% in the ATP/$2e^-$ ratio was observed in the mutant G137E as compared with the W.T. strain; this ratio was improved by 14 and 25% in revertant E137+I147F and revertant E137+N256K, respectively. It is noteworthy that, as expected, when the *bc*1 complex alone is involved, the W.T. strain ATP/$2e^-$ ratio was found to be half of that measured on the whole respiratory chain.

The Transmembrane Potential

The transmembrane electrical potential, $\Delta\Psi$, was measured in the W.T. strain and mutant G137E under the same substrate conditions as above, involving either the whole respiratory chain, the cytochrome oxidase alone, or the *bc*1 complex alone. At the whole respiratory chain level, addition of ethanol to the parental mitochondria led to a 220-mV potential which was broken down to 200 mV upon adding 250 μM ADP and recovered its initial value at a rate which was correlated to the electron transfer activity. In the mutant G137E, adding ethanol led to a 170-mV potential which was broken down to 135 mV upon adding ADP and subsequently recovered completely but very slowly its initial value (Fig.2a). Using D-lactate and oxygen as substrates, the behavior of mutant G137E was very similar to that of the W.T. strain as regards the potential measurements: a potential of roughly 210 mV was measured upon adding D-lactate, which was broken down to 145 mV upon adding ADP and slowly recovered its initial value (Fig. 2b). Lastly, ethanol and ferricyanide were used as substrates in the presence of KCN with a view to determining the potential established by the *bc*1 complex. Under these conditions, the potential was lower in mutant G137E (145 mV) than in the W.T. strain (200 mV). Again, the $\Delta\Psi$ values were found to break down in response to ADP in both the W.T. strain (down to 180 mV) and mutant G137E (down to 110 mV). But, whereas the initial potential value was recovered in the W.T. strain when the steady state 4 was reached, the potential value in the mutant G137E continued to decrease after the breakdown induced by ADP (Fig. 2c).

The transmembrane potential values recorded in revertants E137+I147F and E137+N256K using D-lactate and oxygen as substrates were the same as those determined with the W.T. strain and mutated strains. When the whole respiratory chain or only the *bc*1 complex was involved, the potential values established upon adding ethanol, the breakdown induced by ADP, and the recovery rate up to the initial value were all found to be intermediate between the corresponding parental and mutant values (result shown in Fig. 2a taking the revertant E137+N256k as an example).

Catalytic Efficiency of the *bc*1 Complex for Ubiquinol

The *bc*1 complex can be said to be an enzyme of the ping-pong type (Speck and Margoliash, 1984; degli Esposti and Lenaz, 1991). All the strains studied here exhibited a Michaelis type kinetic behavior, meaning that arrival and binding of DBH2 to its oxidation site were not rate limiting. The experimental $V_{max}/K_m = k_{min}$ value (with V_{max} expressed as the turnover number) gives the apparent second-order constant characteristic of the arrival and binding of the substrate

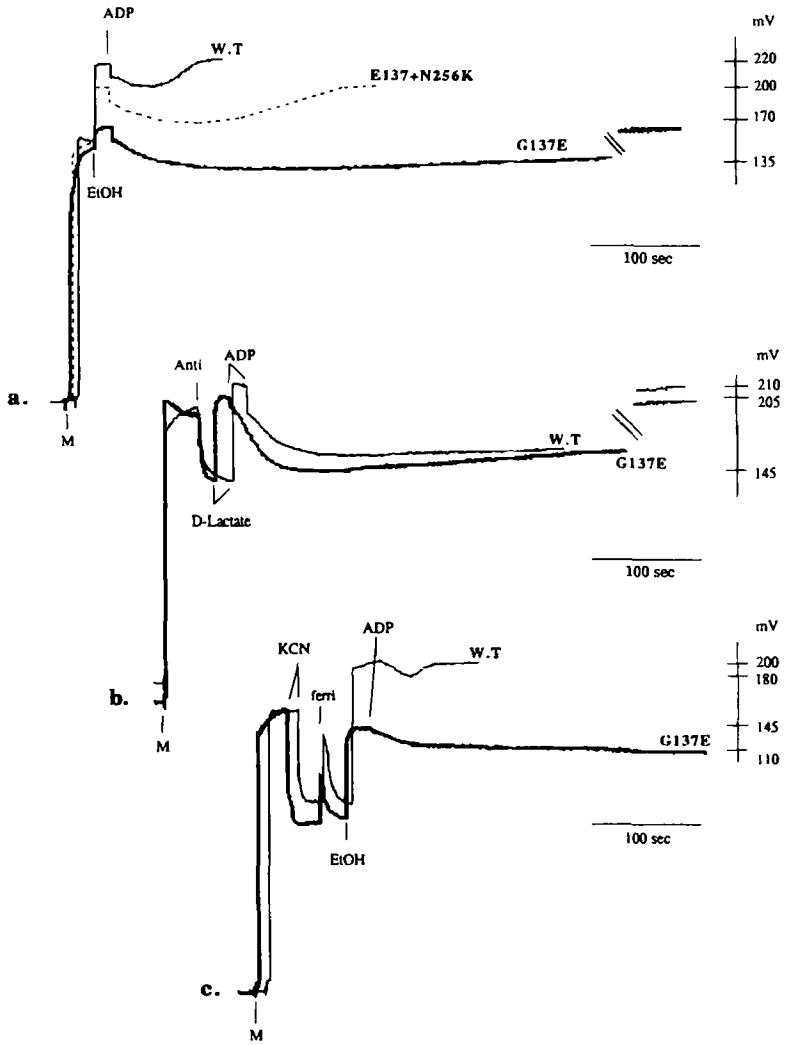

Fig. 2. Mitochondrial transmembranous electrical potential. The transmembrane potential established by the whole respiratory chain. (a) the cytochrome oxidase alone (b), and the *bc*1 complex alone (c) were recorded at 524–499 nm in mitochondria isolated from the wild type strain (W.T.) and the mutant G137E. The mitochondria were diluted to 0.5 mg/ml in 0.65 M manitol, 0.36 mM EDTA, 10 mM Tris-maleate buffer, and 0.3% bovine serum albumin. 1% ethanol, 10 mM D-lactate, 0.25 mM ADP, and 1 mM ferricyanide were used.

to its site. The G137E mutation was found to affect the k_{min} value by less than one order of magnitude, whereas no significant effects were observed on revertants G137E+I147F, G137E+C133S, and G137E+N256K (Table III).

Cytochrome *b* Reduction through Center P and N

Cytochrome *b* was reduced by succinate through center P in the presence of antimycin A and through center N in the presence of myxothiazol. In all the strains, the cytochrome *b* reduction kinetics through center N was found to be slower when DBH2 was used as substrate than with succinate. This probably indicates that the natural Q6 type quinone, which is involved when succinate is used, was a more efficient electron donor than DBH2. The kinetics were recorded at 562 nm vs. 575 nm in mitochondria isolated from the W.T. strain, the mutant and the revertants using the glass bead preparation method. It is noteworthy that the kinetics of these two pathways give a global presteady-state cytochrome *b* reduction value which

Table III. Catalytic Properties of the Ubiquinol-Cytochrome *c* Reductase[a]

Strains	V_m (sec^{-1})	K_m DBH_2 (μM)	k_{min} ($M^{-1}.sec^{-1}$)
W.T. (G137)	65 ± 12.5	15.6 ± 1.3	4×10^6
G137E	19.4 ± 3.5	14 ± 1	1.4×10^6
E137+I147F	20.5 ± 4.5	3.9 ± 0.7	5.2×10^6
E137+C133S	28	8.3	3.4×10^6
E137+N256K	22.5 ± 2.5	7.1 ± 0.2	3.2×10^6

[a] The DBH_2-cytochrome *c* reductase activity was measured in mitochondria isolated from the parental wild type strain (W.T.), mutant strain G137E, and revertants E137+I147F, E137+C133S, and E137+N256K. The reductase activity was measured using 40 μM cytochrome *c*. The V_m values are expressed in turnover numbers (mol cyt. *c* reduced·$mole^{-1}$ cyt.*b*·sec^{-1}). The experimental k_{min} (V_m/K_m) value corresponds to the apparent kinetic second-order constant of the arrival and binding of the substrate to its site.

includes (1) the rate of arrival and binding of the substrate to its site, (2) the rate of the various electron transfer steps occurring between this binding site and cytochrome *b*. The G137E mutation slows down the cytochrome *b* reduction through center P, whereas the secondary mutations either partially (C133S) or completely (I147F and N256K) restore the kinetic observed in the W.T. strain (Fig. 3a). The cytochrome *b* reduction through center N is also affected by the G137E mutation, although to a lesser extent than the reduction through center P; the C133S and N256K secondary mutations almost totally cancel the effects of the G137E mutation, whereas the I147F secondary mutation does not (Fig. 3b).

DISCUSSION

In this study, we analyzed the yeast cytochrome *b* mutant G137E (Tron and Lemesle-Meunier, 1990) and three respiratory sufficient revertants of this nonfunctional mutant in which the wild type sequence is not restored (di Rago *et al.*, 1990a,b). The initial mutation is located on the positive side of the membrane, at the C-terminal part of the cytochrome *b* helix 3 which connects the two heme binding helices 2 and 4. The secondary mutations are located at the level of either adjacent or distal sites: the C133S suppressor mutation is located on helix 3, inside the membrane, whereas the two other I147F and N256K suppressor mutations are extramembranous and are located in loops 3–4 and 5–6, respectively (Fig. 4). The mutant G137E is unable to grow on respiratory substrate but its electron transfer activity is partly conserved at the cellular as well as at the mitochondrial level (Tron and Lemesle-Meunier, 1990; this work). The suppressor mutations restore the respiratory growth in variable

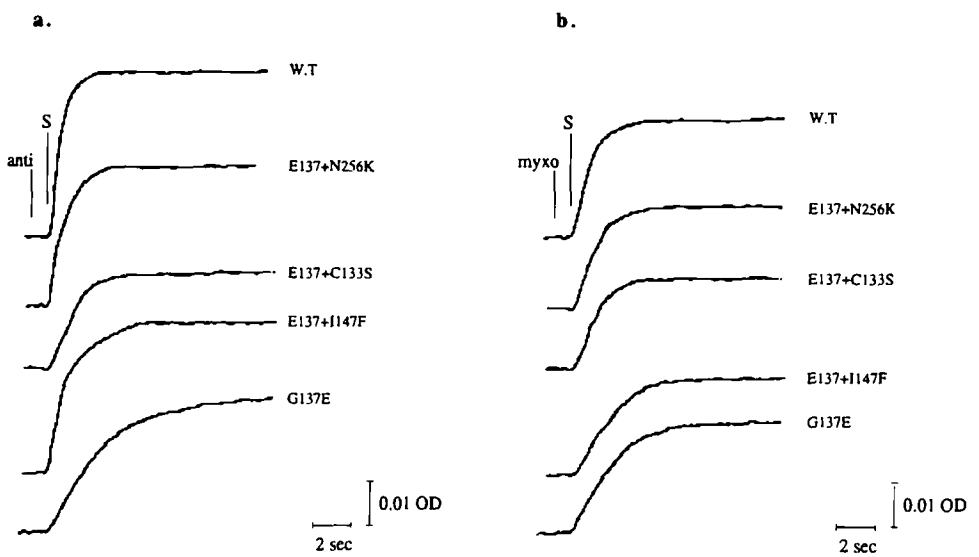

Fig. 3. Reduction of cytochrome b through center P and center N. Reduction of cytochrome *b* by succinate (S) in the presence of antimycin A (a) or myxothiazol (b) was recorded at 562–575 nm. The mitochondrial membranes were prepared from the wild type strain (W.T.), mutant G137E, and revertants E137 + C133S, E137 + I147F, and E137 + N256K. The membranes were diluted to 0.5 μM cytochrome *b* in 0.65 M sorbitol, 10 mM KH_2PO_4, 2 mM EDTA, 0.1 mM $MgCl_2$, and 0.3% bovine serum albumin, pH 6.5.

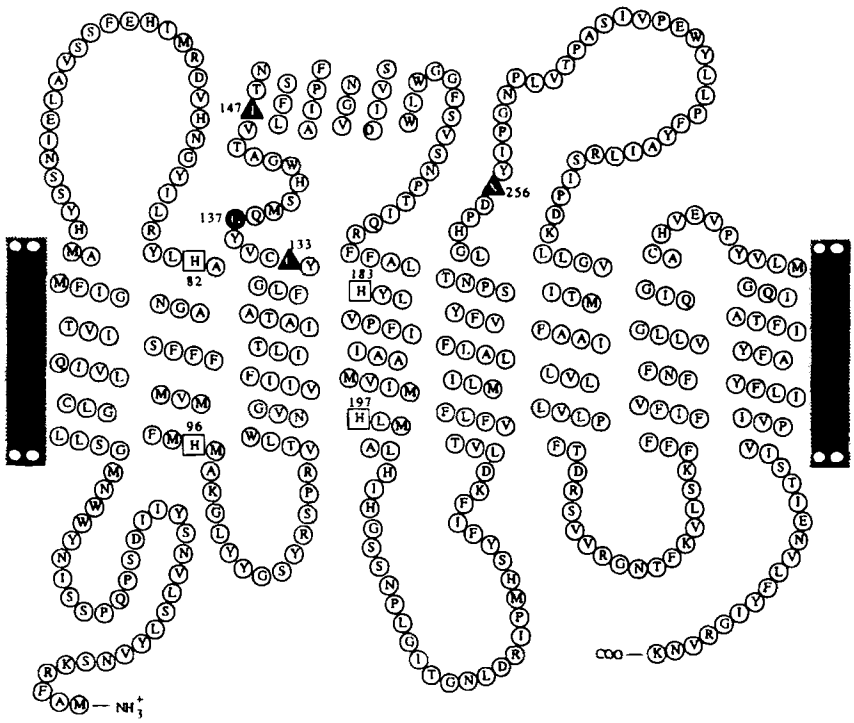

Fig. 4. Secondary structure of *S. cerevisiae* cytochrome *b*. Predicted diagram of the eight membrane-spanning α helix cytochrome *b* (Crofts *et al.*, 1987; Brasseur, 1988). The four conserved histidines, thought to be the ligands to the two heme groups, are shown in open boxes. The hemes bL and bH are predicted to be coordinated to histidines 82 and 183 and to histidines 96 and 197, respectively. Glycine 137 (●), isoleucine 147 (▲), cysteine 133 (▲), and asparagine 256 (▲) are located on the positive side of the inner mitochondrial membrane and are shaded in black.

degrees, although they result in only a slight increase in the various electron transfer activities (Table I). All these strains exhibited low yield in oxidative phosphorylation (phosphorylation efficiency varying from 12 to 42% as regards the wild type strain), indicating an incomplete transduction of the redox energy available in reduced substrates into a displacement from equilibrium of the ATP⇔ADP+Pi reaction. The combination of the very similar electron transfer activities and the differences in ATP production between the three revertants may explain why they grow on respiratory substrates with variable growth rates (the growth rate depends on the ATP produced per weigth and time unit, which is the product of the overall activity of the electron transfer chain by the corresponding P/O).

Replacing glycine by glutamic acid in position 137 decreases the electron transfer activity catalyzed by the *bc*1 complex (Bruel and Lemesle-Meunier, 1993; Giessler *et al.*, 1994; this paper) but does not, or slightly, affect the catalytic efficiency of the complex for DBH2, as shown by the k_{min} value (Table III). The secondary I147F, C133S, and N256K mutations improve the electron transfer activity when compared to the mutant strain and cancel the slight negative effect of the G137E mutation on the *bc*1 complex catalytic efficiency. These results suggest that G137 may weakly interfere with the ubiquinol binding site but rather interfere with some of the intra- or intermolecular electron transfer steps occurring within the *bc*1 complex. Actually, the G137E mutation was found to lead to a decrease in the kinetics of the two cytochrome *b* oxido-reduction pathways, having a greater effects on the center P than on the center N pathway. The secondary mutations partly restore these two electron transfer pathways. It is noteworthy that the kinetics of these two pathways are less greatly affected by the various mutations than the steady-state electron transfer at the ubiquinol-cytochrome *c* reductase and ethanol oxidase activity levels (Table I and Fig. 3). Thus, the perturbation induced by the various mutations is stronger under multiple than single turnover conditions. In the framework of the catalytic switch model

(Brandt and von Jagow, 1991), these results could be taken to mean that the trigger back from the *b* state to the FeS state might be impaired by these mutations. Another possibility might be that the cytochrome *b* reoxidation kinetics at center N becomes the limiting step in the steady-state ubiquinol-cytochrome *c* reductase activity. This explanation is not, however, very plausible since it would imply that the center P located mutations have a stronger effect at center N than at center P.

Replacing glycine in position 137 by glutamic acid makes the mutated strain resistant toward myxothiazol. This resistance is conserved in double mutant E137+N256K, whereas double mutant E137+C133S exhibits a four times lower resistance to myxothiazol than mutant G137E.

Mutant G137E and its revertants exhibit a striking phenotype involving the absence or slow growth on nonfermentable carbon sources despite the retention of a relatively high electron transfer rate at the level of the whole respiratory chain. The data obtained here on the ATP synthesis associated with the electron transfer activity (ATP/$2e^-$ ratio), at the level of the cytochrome oxidase, at that of the *bc*1 complex, and at that of the whole respiratory chain, provided some important insights about this phenotype. Mutation G137E induces a partial decoupling at the *bc*1 level (ATP/$2e^-$ = 50% of the W.T. value), whereas the energetic capacity of the cytochrome oxidase is conserved; the coupling of the whole respiratory chain is also affected. Secondary mutations C133S, I147F, and N256K partly restore the coupling of the *bc*1 complex (ATP/$2e^-$ = 70–80% of the W.T. value) and also increase the overall ATP/$2e^-$ ratio as compared with the mutant strain; the coupling of the cytochrome oxidase is not modified by the secondary mutations. The fact that the cytochrome oxidase coupling properties are not modified by the various mutations indicates that the decoupling observed at the respiratory level as a whole occurs only when the *bc*1 complex is active.

A decrease in the ATP/$2e^-$ ratio means that either the H^+/e^- or the H^+/ATP stochiometry is modified, and hence that either the ATP/$2e^-$ ratio decreased or the H^+/ATP ratio increased. Is an increase in the H^+/ATP stochiometry (ATPase proton slip) possible in these mutants? This seems unlikely for, at least, two reasons: (1) If the ATP synthetase was perturbed in our mutants, a decrease in the P/O ratios would also be expected to occur at the cytochrome oxidase level; but this was not the case in our mutants. Besides, the H^+ATP hydrolase activities measured in the W.T. and the G137E mutated strains were found to be identical (results not shown). (2) It is difficult to explain how point mutations in the cytochrome *b* protein might induce an increase of the H^+/ATP stochiometry. One possibility might be the existence of an ATPase proton slip at low electron transfer rates, but in *S. cerevisiae*, an increase in the ATP/$2e^-$ ratio has been observed at low electron flux level, due to an increase in the $H^+/2e^-$ ratio, while the H^+/ATP ratio remained constant (Ouhabi *et al.*, 1989). These arguments, especially the first one, strongly support the idea that no change in the H^+/ATP stochiometry occurs in the mutants studied. The decrease in the ATP/$2e^-$ ratio observed in the mutated strains can therefore be attributed to a decoupling between the electron transfer and the proton translocation (decrease in the H^+/e^- ratio) within the *bc*1 complex.

In agreement with the ATP/$2e^-$ results, the transmembrane potential values were found to be lower in the case of the mutant than in the case of the W.T. strain in respiratory state 2 and to collapse more strongly with the mutant than with the W.T. strain upon the addition of ADP: this was observed at the whole electron transfer chain level as well as at the *bc*1 complex level. The revertants exhibited intermediate behaviors between that of the mutant and that of the W.T. strain. When, on the contrary, only cytochrome oxidase was functioning, the transmembrane potential values obtained with the mutant, the revertants, and the wild type strain were all found to be identical. These results show that the electrical component of the protonmotive force is impaired in the *bc*1 complex and suggest that the electro- or protogenic reactions at work in this complex have been affected by the mutation.

Three mechanisms have been proposed to account for this energetic decoupling: the proton leak, the redox slip, and the proton slip (for review see Murphy, 1989) (Fig. 5). In the case of our decoupled mutant/revertant strains, the proton leak hypothesis can be ruled out since the ATP/$2e^-$ and transmembrane potential values associated with the cytochrome oxidase were identical to those obtained on the W.T. strain. In the framework of the Q-cycle, which is now a widely accepted model, a redox slip could only result from an impairment of the center P located divergent oxidation of ubiquinol which would lead to the reduction of only the FeS cluster instead of the concerted reduction of the FeS cluster and of *b*L heme; this hypothesis has been previously proposed to explain the DCCD induced decoupling (Beattie, 1993). In this case, the H^+/e^- stochiometry would decrease by exactly 50% and the

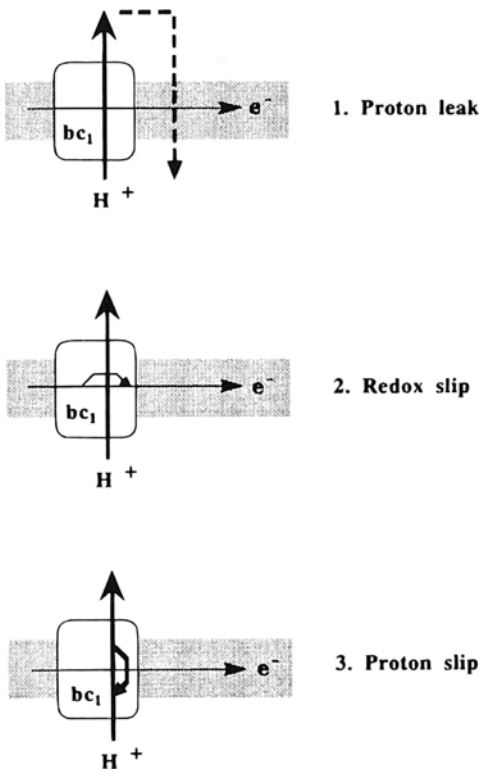

Fig. 5. Possible energetic-decoupling mechanisms. Three energy-decoupling mechanisms have been proposed: the proton leak in which the protons are assumed to passively return to the mitochondrial matrix without any ATP synthesis, the redox-slip mechanism where an electron transfer is assumed not to be coupled to a proton ejection, and the proton-slip mechanism whereby the protons are assumed to come back through the proton pump without any reverse electron transfer or ATP synthesis (Murphy, 1989).

center N would not be functional. Mutant G137E was found to bind antimycin A with the same affinity as the wild type strain and to have the same number of fixation sites (Tron and Lemesle-Meunier, 1990), the ubiquinol-cytochrome *c* reductase activity was completely inhibited by this inhibitor, and the cytochrome *b* reduction kinetic studies showed that both center P and center N are still functional in mutant G137E (Fig. 3). Besides, different ATP/$2e^-$ ratios (varying from 43 to 66% with regard to the W.T. strain) were obtained at the *bc*1 complex level in the various revertants, which indicates that different *bc*1 complex H^+/e^- stochiometries were induced by the various mutations. This particular redox slip model therefore does not account for the partial decoupling we observed in our mutant/revertants. In the proton slip mechanism, the protons pass back down the proton gradient through the proton pump without any reverse electron transfer or ATP synthesis. Contrary to what occurs in the proton leak model, the proton return occurs via a specific protein. Our experimental results are in agreement with the proton slip model; in other words, replacing the nonpolar amino acid glycine in position 137 by the charged glutamic acid residue would result in some protons crossing back through the membrane via the *bc*1 complex when it is functioning.

How are these phenomenological results to be interpreted in terms of molecular mechanism? Protons move through a lattice via closely related points, the hop distance being less than 1 Å. Two models for long-range proton translocation through a membrane embedded protein have been proposed: the so-called H.B.C. model in which the proton translocation network uses a hydrogen-bound chain (H.B.C.) consisting of protonic amino acids (Onsager, 1969; Nagle and Tristram-Nagle, 1983); and a second model based on the property of a protein to be transiently accessible to water, depending on its structure fluctuation (a fast process occurring in the millisecond range) (Woodward *et al.*, 1982). The two processes assumed to occur in these models might operate simultaneously to induce proton wires (Nagle and Morowitz, 1978; Nagle and Tristram-Nagle, 1983) which may involve either an interaction between various helices within a protein [as in bacteriorhodopsin (Rothschild, 1992)] or the protein–protein interaction inside the membrane, or the protein–lipid interface (Murphy, 1989). In the *bc*1 complex, protonation/deprotonation of the quinol/semiquinone and quinone/semiquinone couples occurs at centers P and N, respectively, and the protons move from these sites to the bulk phase (and conversely) via unknown pathways. Among the 900 known cytochrome *b* sequences (degli Esposti *et al.*, 1993), 14 protonic amino acid residues are completely conserved and might be involved in the hydrogen chains along which the proton could move; however, some of them (S87 and E272) seem to play no role in hydrogen bonding, as shown by site-directed mutagenesis experiments (Yun *et al.*, 1992; Crofts *et al.*, 1992). Among these protonic acid residues, nine are located inside the membrane, including the four heme-coordinating histidines. The number of protonic amino acid residues is therefore obviously insufficient for the movement of the protons through the membrane only via a H.B.C. mechanism. If any such movement occurred, it would involve the various modes of proton movement that constitute the proton wire described above.

Our results suggest that replacing glycine by glutamic acid in position 137 must lead to a conformational and/or a local pH and/or a local ionic strength

change at center P inducing a change of the proton route. When the *bc*1 complex is functioning, some of the protons released at center P, instead of taking the proton wire route which leads to the P bulk phase, might follow another proton wire which leads to the N bulk phase (decoupling proton wire); a model on these lines has been proposed (Brandt and Trumpower, 1994) as an alternative explanation for the protonmotive Q cycle decoupling induced by DCCD (Beattie *et al.*, 1984; Beattie and Marcelo-Baciu, 1991) and as an explanation for our findings that some mutants which did not grow on respiratory substrate continued to show some electron transfer activity (Tron and Lemesle-Meunier, 1990; Lemesle-Meunier *et al.*, 1993); on the other hand, Miki *et al.* (1994) have postulated that the DCCD inhibited membrane potential linked reverse electron transport in the *bc*1 complex is closely coupled to a reverse flow of protons presumably through a proton channel significantly involving the cytochrome *b* subunit. The results obtained here on the revertants show the existence of an ATP/$2e^-$ ratio which was intermediate between that of the G137E mutant and that of the W.T. strain, which indicates that the two proton wires may coexist. Our results suggest that the decoupling proton wire may not be a permanent structure but rather a dynamic (and directionally controlled) structure requiring an active *bc*1 complex; only the protons released by a currently functioning complex can take this proton wire and return to the N side of the membrane. This corresponds to a proton slip which is compatible with the protonmotive Q cycle model. A potential decoupling proton wire may in fact exist in the functioning wild type *bc*1 structure. This proton wire might be variably effective depending on the electron flux conditions and might be largely uncovered by some mutations. The variable stochiometry observed in the yeast *S. cerevisiae bc*1 complex, under different electron flux values (Ouhabi *et al.*, 1989), might be attributable to the existence of a proton wire. A proton wire would also explain why the N side located S206L mutation (in the loop connecting helices 4 and 5) leads to the same decoupling effects as the mutation G137E: mutant S206L does not grow on respiratory substrate although it exhibits a relatively high electron transfer activity (Lemesle-Meunier *et al.*, 1993), and the ATP/$2e^-$ ratio obtained using ethanol and oxygen as substrates was only 50% of that of the W.T. strain (unpublished results). This mutant exhibits an apparently functional QP site and an impaired QN site, indicating that the environment of the heme *b*562 group has undergone a change (Lemesle-Meunier *et al.*, 1993). It is possible that mutation S206L may uncover the pre-existing proton wire when the *bc*1 complex is functioning, as does the G137E mutation.

In conclusion, our results show that a partial decoupling of the *bc*1 complex is induced by the cytochrome *b* point mutation G137E which affects a residue located in the QP domain. The decoupling is partly compensated for by three different secondary mutations and can be explained in terms of the existence of a proton wire connecting centers P and N in the wild type *bc*1 complex, which may be amplified and/or uncovered by the G137E mutation when the protonmotive Q cycle is functioning; this proton wire may constitute the molecular basis of a proton slip.

ACKNOWLEDGMENTS

We thank P. P. Slonimski and J. P. di Rago for providing us with mutant, revertants, and wild type strain. We are grateful to M. Rigoulet for helpful discussion. We also acknowledge S. Raymond for technical assistance and J. Blanc for english revision. This research was supported by a grant from the European Commission of Communities (Contract SCI-0010C-C).

REFERENCES

Beattie, D. S. (1993). *Eur. J. Biochem.* **25**, 233–244.
Beattie, D. S., and Clejan, L. (1982). *FEBS Lett.* **149**, 245–248.
Beattie, D. S., and Marcelo-Baciu, R. M. (1991). *J. Bioenerg. Biomembr.* **23**, 665–679.
Beattie, D. S., and Villalobo, A. (1982). *J. Biol. Chem.* **256**, 14745–14752.
Beattie, D. S., Clejan, L., and Bosch, C. G. (1984). *J. Biol. Chem.* **259**, 10526–10532.
Brandt, U., and Trumpower, B. (1994). *Crit. Rev. Biochem. Mol. Biol.* **29**, 165–197.
Brandt, U., and von Jagow, G. (1991). *Eur. J. Biochem.* **195**, 163–170.
Brasseur, R. (1988). *J. Biol. Chem.* **263**, 12571–12575.
Bruel, C., and Lemesle-Meunier, D. (1993). *Biochem. Soc. Trans.* **22**, 61S.
Chevillotte-Brivet, P., and Meunier-Lemesle, D. (1980). *Eur. J. Biochem.* **111**, 161–169.
Clejan, L., and Beattie, D. S. (1983). *J. Biol. Chem.* **258**, 14271–14275.
Coppée, J.-Y., Brasseur, G., Brivet-Chevillotte, P., and Colson, A.-M. (1994). *J. Biol. Chem.* **269**, 4221–4226.
Crofts, A. R. (1985). In *The Enzymes of Biological Membranes* (Martonosi, A., ed), Plenum Press, New York, pp. 347–382.
Crofts, A. R., and Wraight (1983). *Biochim. Biophys. Acta* **726**, 149–185.
Crofts, A. R., Robinson, H., Andrews, K., Doren, S. V., and Berry, E. (1987). In *Cytochrome Systems* (Papa, S., Chance, B., and Ernster, L., eds.) Plenum Press, New York, pp. 617–624.
Crofts, A., Hacker, B., Barquera, B., Yun, C.-H., and Gennis, R. (1992). *Biochim. Biophys. Acta* **1101**, 162–165.
degli Esposti, M. (1983). *Biochim. Biophys. Acta* **725**, 349–360.

degli Esposti, M., and Lenaz, G. (1991). *Arch. Biochem. Biophys.* **289**, 303–312.
degli Esposti, M., Vries, S. D., Crimi, M., Ghelli, A., Patarnello, T., and Meyer, A. (1993). *Biochim. Biophys. Acta* **1143**, 243–271.
di Rago, J.-P., Netter, P., and Slonimski, P. P. (1990a). *J. Biol. Chem.* **265**, 3332–3339.
di Rago, J.-P., Netter, P., and Slonimski, P. P. (1990b). *J. Biol. Chem.* **265**, 15750–15757.
Emaus, R. K., Grunwald, R., and Lemasters, J. L. (1986). *Biochim. Biophys. Acta* **850**, 426–448.
Giessler, A., Geier, B., di Rago, J.-P., Slonimski, P. P., and von Jagow, G. (1994). *Eur. J. Biochem.* **222**, 147–154.
Guérin, B., Labbe, P., and Somlo, M. (1979). *Methods Enzymol.* **55**, 149–159.
Kotylak, Z., and Slonimski, P. P. (1977). In *Mitochondria: Genetics and Biogenesis of Mitochondria* (Bandlow, W., Schweyen, R. J., Wolf, K., and Kaudewitz, F., eds.), Walter de Gruyter, Berlin, pp. 161–172.
Kovac, L., Lachowicz, T. M., and Slonimski, P. P. (1967). *Science* **158**, 1564–1567.
Lemesle-Meunier, D., Brivet-Chevillotte, P., di Rago, J. P., Slonimski, P. P., Bruel, C., Tron, T., and Forget, N. (1993). *J. Biol. Chem.* **268**, 15626–15632.
Link, T. A., Haase, U., Brandt, U., and von Jagow, G. (1993). *J. Bioenerg. Biomembr.* **25**, 221–232.
Meunier-Lemesle, D., Chevillotte-Brivet, P., and Pajot, P. (1980). *Eur. J. Biochem.* **111**, 151–160.
Miki, T., Miki, M., and Orii, Y. (1994). *J. Biol. Chem.* **269**, 1827–1833.
Mitchell, P. (1975). *FEBS Lett.* **59**, 137–139.
Mitchell, P. (1976). *J. Theor. Biol.* **62**, 327–367.
Murphy, M. P. (1989). *Biochim. Biophys. Acta* **977**, 123–141.
Nagle, J. F., and Morowitz, H. J. (1978). *Proc. Natl. Acad. Sci. USA* **75**, 298–302.
Nagle, J. F., and Tristram-Nagle, S. (1983). *J. Membr. Biol.* **74**, 1–14.
Ohnishi, T., Kawaguchi, K., and Hagihara, B. (1966). *J. Biol. Chem.* **241**, 1797–1807.
Onsager, L. (1969). *Science* **166**, 1359–1364.
Ouhabi, R., Rigoulet, M., and Guerin, B. (1989). *FEBS Lett.* **254**, 199–202.
Rao, J. K. M., and Argos, P. (1986). *Biochim. Biophys. Acta* **869**, 197–214.
Rothschild, K. J. (1992). *J. Bioenerg. Biomembr.* **1**, 147–167.
Speck, S. H., and Margoliash, E. (1984). *J. Biol. Chem.* **259**, 1064–1072.
Sujino, Y., and Miyoshi, Y. (1964). *J. Biol. Chem.* **239**, 2360–2364.
Tron, T., and Lemesle-Meunier, D. (1990). *Curr. Genet.* **18**, 413–419.
Trumpower, B. L. (1990a). *J. Biol. Chem.* **265**, 11409–11412.
Trumpower, B. L. (1990b). *Microbiol. Rev.* **54**, 101–129.
Wang, Y., and Beattie, D. S. (1991). *Arch. Biochem. Biophys.* **291**, 363–370.
Woodward, C., Simon, I., and Tuchsen, E. (1982). *Mol. Cell. Biochem.* **48**, 135–160.
Yang, M., and Trumpower, B. L. (1986). *J. Biol. Chem.* **261**, 12282–12289.
Yang, M., and Trumpower, B. L. (1988). *J. Biol. Chem.* **263**, 11962–11970.
Yun, C.-H., Wang, Z., Crofts, A. R., and Gennis, R. B. (1992). *J. Biol. Chem.* **267**, 5901–5909.